Broadband Time-Domain Measurement System applied to the Characterization of Cross-Modulation in Nonlinear Microwave Devices.

M. Abouchahine, A. Saleh, G. Neveux, T. Reveyrand, J.P. Teyssier, D. Barataud, and J. M. Nebus

University of Limoges, XLIM, UMR n°6172, 123 Av. A. THOMAS, 87060 LIMOGES Cedex, France

***Abstract* — This paper presents a calibrated 4 channel broadband time-domain measurement system for the characterization of nonlinear microwave devices. The hardware architecture of the proposed measurement system is described with particular emphasis on the samplers and Intermediate Frequency (IF) circuit configuration. The sampling heads are working at a high strobe signal repetition frequency that can be tuned between 357MHz and 536MHz. 40 GHz RF frequency bandwidth is achieved. The calibration procedure of this system is also described. This instrument is then used for cross-modulation characterization of a 15W GaN HEMT CREE power amplifier at S Band. Cross-modulation measurements between a double side band amplitude modulation and a single tone signal at a 60MHz offset frequency are performed to illustrate the capabilities of the proposed system. Time-domain waveforms are measured and variations of amplitude and phase modulation indices versus input power are recorded.**

***Index Terms* — cross-modulation (CM), Nonlinear microwave circuits, GaN power amplifiers, Time-domain measurements.**

I. Introduction

Wide band communication systems are increasingly being required to target multi-standard and multi-band applications. Various architecture design solutions as well as different modulation standards and multiple access techniques can be implemented [1], [2]. Due to non ideal frequency isolation between the transmitter and the receiver, Tx leakage signals could create interferences and cross-modulation with the Rx useful signal resulting in reduced Signal to Noise Ratio (SNR) and ultimately, degradations in system performance [3].

Cross-modulation in nonlinear devices has been theoretically studied and simulations using behavioral modeling techniques have been reported [4], [5]. The work proposed in this paper covers complementary aspects as it focuses on a measurement technique and setup. Cross-modulation characterization and its impact on Adjacent Channel Power Ratio (ACPR) or Adjacent Channel Leakage ratio (ACLR) have been performed using spectrum analyzer techniques [6], [7]. In this paper a time-domain measurement approach based on wideband harmonic sub-sampling principle is proposed.

Recently, different time-domain measurement systems have been proposed to perform large bandwidth characterization of nonlinear microwave devices. The need for a good trade off between dynamic range and frequency bandwidth has led to the use of Microwave Transition Analyzer (MTA) [8], Digital Storage Oscilloscopes DSO [9], [10], or Large Signal Analyser (LSNA) [11], [12]. Instruments based on sub-sampling principle have a quite good dynamic range at the detriment of a limited envelope bandwidth (in the order of 10 MHz) due to low frequency repetition rate of the strobe signal. Time-domain measurements of wideband multisines have been performed using the sub-sampling principle of the LSNA and a fine grid (20MHz) calibrated comb generator [13]. Nevertheless, the RF measurement bandwidth was limited to 2 GHz due to a large attenuation of high frequency spectral components generated by the comb generator. To reach broadband performances, specific processing techniques have also been proposed to descramble and to stitch the downconverted RF spectrum in a limited 10 MHz IF bandwidth [12], [13]. The complexity of such post processing or the need for specific phase standards are due to the hardware frequency limitation of sampling heads.

In this paper, we propose a new architecture based on the use of sampling heads working with a high repetition frequency strobe signal (from 350MHz to 540 MHz). In the first part of this paper, the architecture of the proposed test-set that we have built, is described. RF and envelope bandwidths are highlighted. In the second part, the calibration procedure of the test bench is explained. In the third part, cross-modulation measurements at S Band performed on a 15W GaN HEMT CREE power amplifier are reported to demonstrate potential capabilities of the measurement system. To conclude, comments concerning future enhancements are mentioned.

II. Description of the Measurement System.

A. Hardware configuration for wideband measurements.

The proposed instrument is based on the sub-sampling principle which enables downconversion of microwave spectra into IF spectra. The downconvertor is the key component of the instrument. The key feature presented here to enable waveform measurements of broadband modulated signal is the use of a strobe signal having a high frequency

repetition rate. For that purpose, dual sampler parts of a VNA have been used and modified to build a new sampling unit configuration as shown in Fig 1.

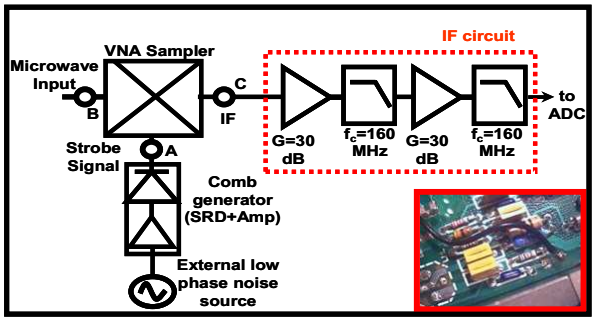

Fig.1. Modified sampling head of the new instrument.

A low phase noise source with a tunable frequency in the 357 MHz – 536 MHz range drives an amplifier and a comb generator based on the use of a Step Recovery Diode. This assembly providing narrow pulses with high repetition rate is used to generate the strobe signal of the sampling head. A RF bandwidth of 40 GHz and a theoretical envelope bandwidth of 270 MHz can be reached. When a CW input microwave signal drives the sampling head, a wide output IF signal spectrum resulting from multiple mixing products is obtained as sketched in fig 2.

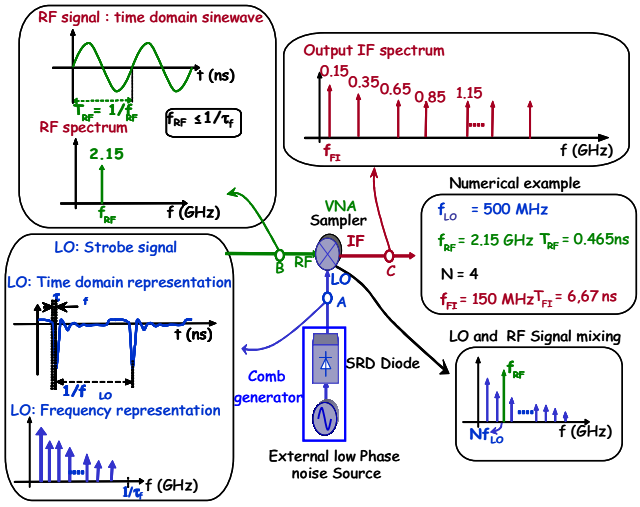

Fig.2. Numerical example of a broadband sub-sampling principle applied to a CW RF signal.

A 160 MHz bandwidth IF stage has been built for signal amplification, anti-aliasing filtering and for adjusting the signal to the full scale of ADCs. For the moment, time-domain data acquisition is achieved by using a 4 channel 1Gs/s sampling scope. The IF stage includes 2 [DC-2GHz] 30dB gain monolithic amplifiers and 2 [DC-160MHz] ceramic low pass filters as indicated in Fig 1. Doing so we got good matching conditions, ensured electrical stability and appropriate signal level for the ADC circuits. The measured conversion gain of the 4 synchronized channel sub-sampling unit versus the RF input frequency is shown in Fig 3.

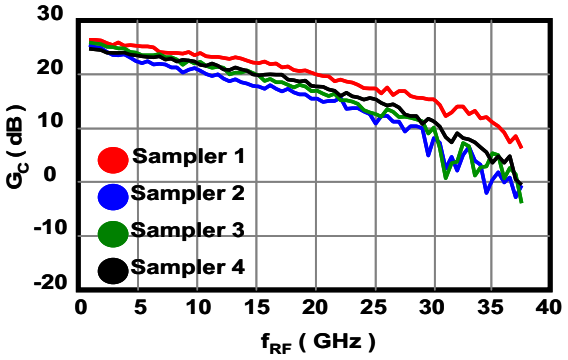

Fig.3. Measured Conversion Gain of the 4 sub-sampling channels.

The whole measurement system sketched in Fig. 4 is fully computer controlled for data acquisition and signal processing (such as FFT and error correction matrix computation).

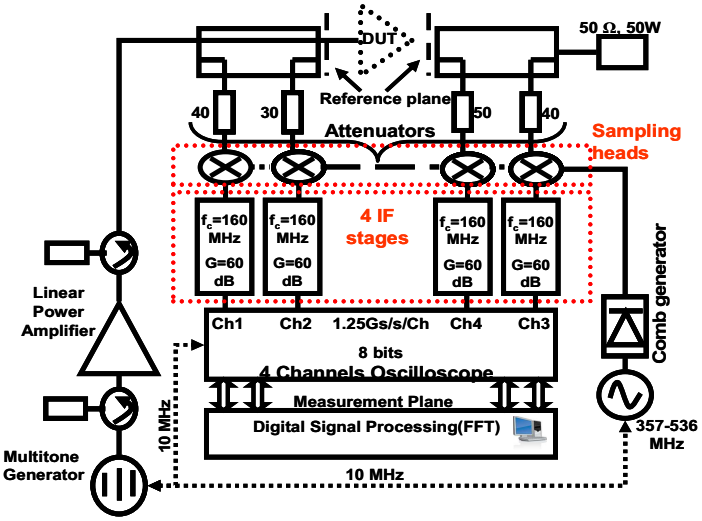

Fig.4 Block diagram of the broadband time-domain measurement set-up.

For the moment the dynamic range is limited to approximatively 50 dB. This is essentially due to the 8 bits sampling scope channels that we use.

B. System calibration procedure

The purpose of the system calibration procedure is to get a matrix of error terms linking raw data provided by scope measurement channels and incident and scattered power waves at the device under test ports.

The error correction matrix [11] is expressed as following:

$$\begin{bmatrix} a_1^i \\ b_1^i \\ a_2^i \\ b_2^i \end{bmatrix}_{DST} = K^i \exp(j\varphi^i) \begin{bmatrix} 1 & \beta_1^i & 0 & 0 \\ \gamma_1^i & \delta_1^i & 0 & 0 \\ 0 & 0 & \alpha_2^i & \beta_2^i \\ 0 & 0 & \gamma_2^i & \delta_2^i \end{bmatrix} \begin{bmatrix} a_{1M}^i \\ b_{1M}^i \\ a_{2M}^i \\ b_{2M}^i \end{bmatrix} \quad (1)$$

i: denotes frequency index.

In a first step, a classical SOLT calibration is made to determine all error terms except K^i and φ^i. Then, in a second step, a power calibration is done at a relatively high 30 dBm power by using a power sensor and a calibrated 20 dB attenuator. At the end of this step K^i coefficients are determined. After that, a phase calibration is performed in order to determine φ^i coefficients. For that purpose, we used a commercially available Signal Modulation Unit (SMU) which provides multi-sine signal having a maximum bandwidth of 80 MHz. 70 tone signal with 1MHz frequency spacing and known amplitude and phase relationships is used as our standard phase reference signal. The shape of this signal spectrum is shown in Fig. 5.

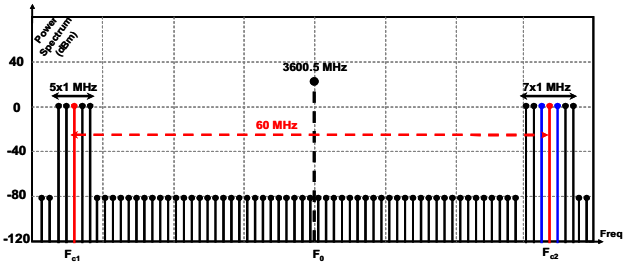

Fig.5. Spectrum shape of phase reference signal.

III. Application to Broadband Cross-Modulation Measurements

In this third part, the proposed measurement system is applied to cross-modulation effect measurements. A 15W, -16 dB gain, - S Band,- 50 Ω matched GaN HEMT CREE power amplifier is driven simultaneously by two signals: a large signal amplitude modulated carrier (31,6% modulation index) at 3.63 GHz (f_{c2}), and a low level CW non modulated carrier at a 60 MHz offset frequency (f_{c1}).

Fig. 6 represents the measured and corrected output spectrum of the amplifier when driven in its nonlinear region (compression zone). This corresponds to the classical frequency illustration of the cross-modulation phenomenon.

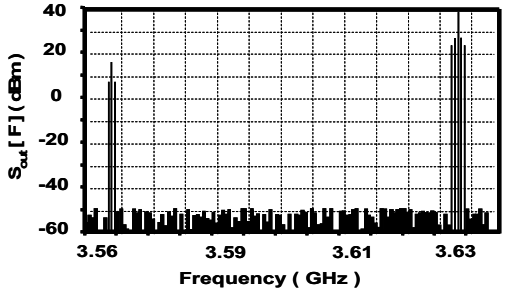

Fig.6. Corrected output power spectrum for $P_{in}(f_{c2})$=31.9 dBm (compression zone).

Fig 7 shows an image of the time-equivalent measured non-constant envelope output current waveforms (the amplifier is 50 Ω loaded) of the modulated signal at f_{c2}.

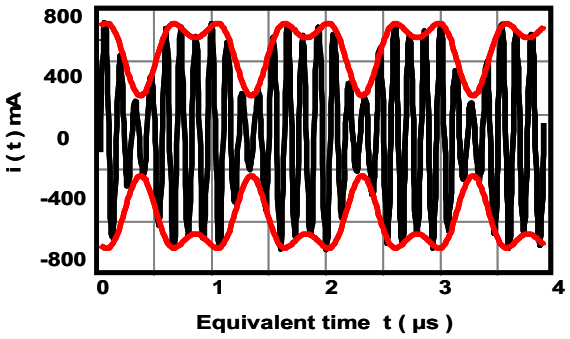

Fig.7. Time-domain current waveform around f_{c2} of TX leakage for $P_{in}(f_{c2})$= 31.9 dBm (compression zone).

Fig 8 shows an image of the time-equivalent measured non-constant envelope output current waveforms (the amplifier is 50 Ω loaded) of the cross-modulated low level carrier at f_{c1} equal to 3.57 GHz. Such time-domain curves, recorded at high power driving the AUT input, provide a visual inspection of cross-modulation effects transferred to the f_{c1} offset low level frequency.

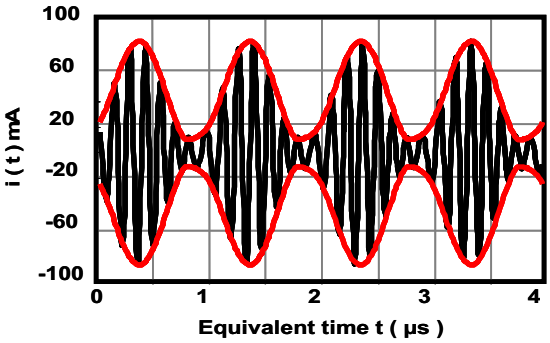

Fig.8. Time-domain current waveform around f_{c1} tone for $P_{in}(f_{c2})$= 31.9 dBm (compression zone).

It is then possible to define amplitude and phase modulation indices of the low level offset carrier at f_{c1}:

$$|Ind_{CM}| = \frac{Max(|Env_{offset\_tone}|) - Min(|Env_{offset\_tone}|)}{Max(|Env_{offset\_tone}|) + Min(|Env_{offset\_tone}|)} \quad (2)$$

$$\angle Ind_{CM} = \frac{Max(\angle(Env_{offset\_tone})) - Min(\angle(Env_{offset\_tone}))}{2} \quad (3)$$

| |Denote the mag of the envelope and ∟ denote the phase of the envelope.

Fig. 9 shows the variations of modulation indices defined in (2) and (3) versus input power driving the device.

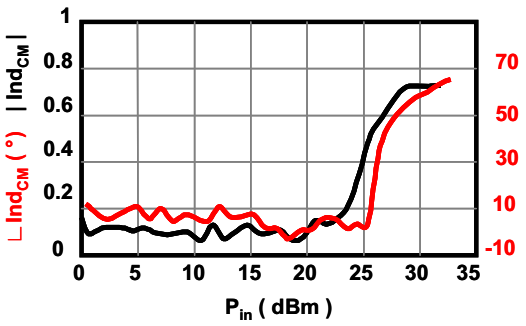

Fig.9. Magnitude and phase voltage modulation index module versus average input power at f_{c1}.

Cross-modulation indices remain to zero when the amplifier works in its linear region and a variation appears when the amplifier is driven into its nonlinear operation regime.

IV. Conclusion

A broadband calibrated 4 channel time-domain measurement system for the characterization of nonlinear devices such as power amplifiers has been presented in this paper. A novel hardware architecture of sampling heads and IF circuits has been proposed to perform large bandwidth time-domain measurements of modulated signals at both ports of power amplifiers.The main further investigations concern the improvement of the dynamic range which is limited to 50 dB in this system.

This characterization tool has demonstrated a valuable capability to aid in characterizing power amplifiers for wideband mobile communication systems and can be applied to other devices such as LNA.

The measurement tool is also expected to be useful for the behavioral modeling of nonlinear devices with memory.

ACKNOWLEDGEMENT

The authors wish to acknowledge Christian Poumier (THALES) for his helpful technical assistance and the "Délégation Générale pour l'armement" for its technical expertise.Research reported here was performed in the context of the ELOPSYS cluster's Lipsys project and supported by the "Ministère de l'économie des finances et de l'emploi Direction Générale des Entreprises" under contract 06.2.93.0716, http://www.elopsys.fr/

REFERENCES

[1] M Sanduleanu., M. Vidojkovic, V.Vidojkovic, A. Van Roermund, A. Tasic, "Receiver front-end circuits for future generations of wireless communications", *2008 IEEE Transactions on Circuits and Systems II: Express Briefs*, vol. 55, Issue 4, pp. 299-303, April 2008.

[2] M. Brandolini, F. Svelto, "Reconfigurable Si RF Receiver Front-Ends for Multi-Standard Radios", *Proc. Of the 1st European Wireless Technology Conference,* pp. 33–36, October 2008.

[3] M. Ranjan, and L. Larson, "An Analysis of cross-modulation distortion in ultra wideband OFDM receivers", *IEEE MTT-S Int. Microw; Symp. Dig.,* pp. 872 – 875, June 2006.

[4] Beom-Kyu Ko, Dong-Bin Cheon, Seong-Wook Kim, Jin-Su Ko, Jeong-Keun Kim, Byeong-Ha Park, "A nightmare for CDMA RF receiver: the cross-modulation", *The First IEEE Asia Pacific Conference on ASICs, 1999. AP-ASIC '9,* pp. 400 – 402, 23-25 Aug. 1999.

[5] Heung-Gyoon Ryu, Heui Seop Byeon, Jin Kwan Kim, "Power spectrum analysis of the cross/intermodulation in the nonlinear LNA", *IEEE Transactions on Vehicular Technology,.* vol. 55, Issue 3, pp. 917-923, May 2006.

[6] H. Pretl, L. Maurer, W. Schelmbauer, R. Weigel, B. Adler, J. Fenk, "Linearity considerations of W-CDMA front-ends for UMTS", *Microwave Symposium Digest., 2000 IEEE MTT-S International,.* vol. 1, pp. 433 - 436, June 2000.

[7] V. Aparin, B. Butler, P. Draxler, "Cross-modulation distortion in CDMA receivers", *Microwave Symposium Digest., 2000 IEEE MTT-S International,.* vol. 3, pp. 1953 - 1956, 11-16 June 2000.

[8] C.J. Clark, G. Chrisikos, M.S. Muha , A.A. Moulthrop and C.P. Silva, "Time-Domain Envelope Measurement Technique with Application to Wideband Power Amplifier Modeling", *IEEE Trans. Microwave Theory and Tech,.* Vol. 46, No. 12, pp. 2531-2540, December 1998

[9] F. Macraigne, T. Reveyrand, C. Maziere, D. Barataud, J.M. Nebus, R. Quere; A. Mallet, "A fully calibrated four channels time-domain RF envelope measurement system for the envelope characterization of nonlinear devices in a load-pull environment", *Microwave Conference, 2005 European,.* Vol. 2, pp. 729-732, 4-6 Oct. 2005

[10] David J. Williams, Jonathan Leckey, Paul J. Tasker, "Envelope Domain Analysis of Measured Time-Domain Voltage and Current Waveforms Provide for Improved Understanding of factors Effecting Linearity", *2003 IEEE MTT-S Int. Microwave Symp* pp. 1411-1414, June 2003.

[11] M. El Yaagoubi, G. Neveux, D.Barataud, T. Reveyrand, J.-M. Nebus, Verbeyst, F.; Gizard, F.; Puech, J, "Time-Domain Calibrated Measurements of Wideband Multisines Using a Large-Signal Network Analyzer", *IEEE Transactions on Microwave Theory and Techniques,* vol. 56, Issue 5, Part 1, pp. 1180 - 1192, May 2008.

[12] W. Van Moer, Y. Rolain, "An improved broadband conversion scheme for the large signal network analyzer", *Microwave Symposium Digest, 2005 IEEE MTT-S International.*, pp. 1501 - 1504, 12-17 June 2005.

[13] M. El Yaagoubi, G. Neveux, D. Barataud, J.M. Nebus, J. Verspecht, "Accurate phase measurements of broadband Multitone signals using a specific configuration of a Large Signal Network Analyzer", *Microwave Symposium Digest, 2006 IEEE MTT-S International.*, pp. 1448 - 1451, June 2006